

Supporting Information

Synthesis of Copper(II) Complex-functionalized Fe₃O₄@ISNA (ISNA=Isonicotinic acid) as magnetically recoverable nanomaterials: Catalytic studies on Alcohol oxidation, Nitrophenol reduction and TD-DFT studies.

Rimpa Mondal^a, Aratrika Chakraborty^b, Ennio Zangrand^c, Madhulata Shukla^d, * and Tanmay Chattopadhyay ^{a,*}

^a Department of Chemistry, Diamond Harbour Women's University, Diamond Harbour Road, Sarisha, South 24 Pgs, 743368

^b Department of Chemistry, Lady Brabourne College, P-1/2 Suhrawardy Avenue, Kolkata 700 017, India

^c Department of Chemical and Pharmaceutical Sciences, University of Trieste, Trieste-34127, Italy

^d Department of Chemistry, Gram Bharti College Ramgarh, Veer Kunwar Singh University, Kaimur-821110, India

INDEX

Fig./Table		Page
Fig. S1	FT-IR spectra of HL^1 . Left, highlighted region is magnified to show the peaks due to C=N frequency [1645 cm^{-1}]; Right, skeletal vibration of aromatic benzene ring [1541 cm^{-1}]	3
Fig. S2	FT-IR spectra of HL^2 . Left, highlighted region is magnified to show the peaks due to C=N frequency [1647 cm^{-1}]; Right, skeletal vibration of aromatic benzene ring [1540 cm^{-1}].	3
Fig. S3	(a) ^1H NMR of 4-chloro-2-(2pyridyl)ethyl)imino)methyl)phenol(HL^1) (b) ^{13}C NMR of 4-chloro-2(2pyridyl)ethyl)imino)methyl)phenol(HL^1).	4
Fig. S4	(a) ^1H NMR of 4-bromo-2(2pyridyl)ethyl)imino)methyl)phenol(HL^2) (b) ^{13}C NMR of 4-bromo-2(2pyridyl)ethyl)imino)methyl)phenol(HL^2).	5
Fig. S5	FT-IR Spectra of Complex 1 $[\text{CuL}^1\text{Cl}]_2$	6
Fig. S6	FT-IR Spectra of Complex 2 $[\text{CuL}^2\text{Cl}]_2$	6
Fig. S7	UV Visible spectra of the ligand and complex 1 $[\text{CuL}^1\text{Cl}]_2$	7
Fig. S8	UV Visible spectra of the ligand and complex 2 $[\text{CuL}^2\text{Cl}]_2$	7
Fig. S9	FT-IR spectra of (a) $\text{Fe}_3\text{O}_4@\text{ISNA}$ (b) magnified portion highlighting FT-IR spectrum of $\text{Fe}_3\text{O}_4@\text{ISNA}$ (c) $\text{Fe}_3\text{O}_4@\text{ISNA}@\text{CuL}^1$	8-9
Fig. S10	The F_{obs} vs F_{calc} plot for complex 1 after suitably processed data	9
Fig. S11	The F_{obs} vs F_{calc} plot for complex 2 .	10
Fig. S12	View of reciprocal lattice for complex 2 .	10
Fig. S13	Few selected different vibrational modes/motions of high intensity for complex 2 .	11
Fig. S14	Correlation of calculated and experimental frequencies of complex 2 .	11
Table 1S	Hydrogen bond parameters ($\text{\AA} / {}^\circ$) for complex 2 .	12
Table 2S	Selected DFT calculated harmonic vibrational frequencies of complex 1 (a scaling factor of 0.96 was used above 2900 cm^{-1}) and of 2 and their band assignments.	12
Table 3S	The calculated absorption maxima, oscillator strength, and their corresponding band assignment for complex 1 .	13
Table 4S	The calculated absorption maxima, oscillator strength, and their corresponding band assignment for complex 2 .	13

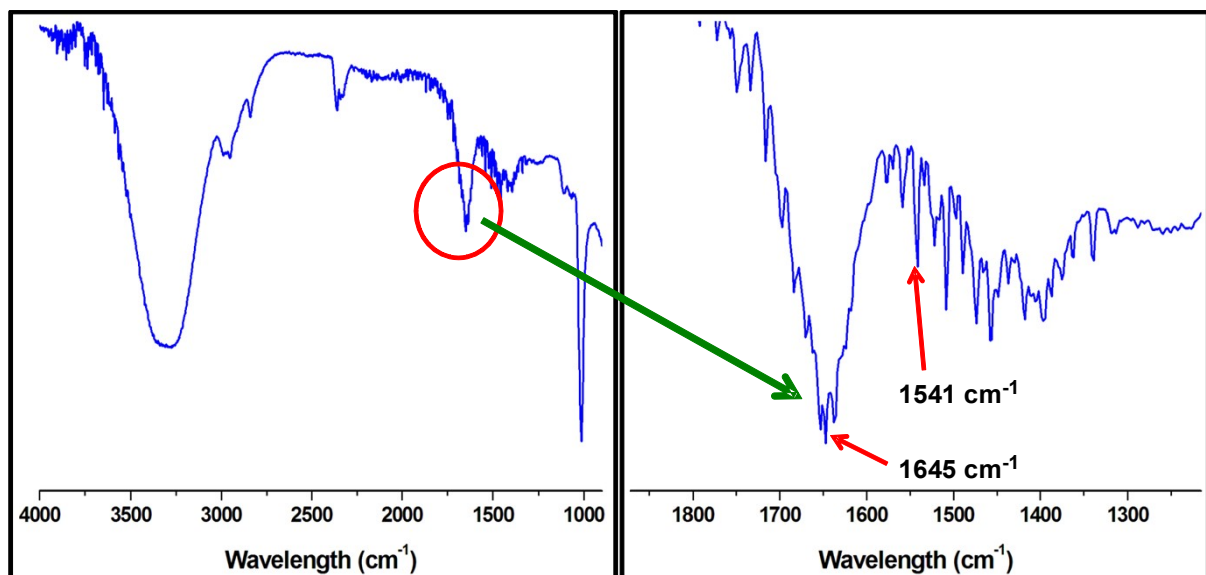


Fig. S1. FT-IR spectra of HL¹. Left, highlighted region is magnified to show the peaks due to C=N frequency [1645 cm⁻¹]; Right, skeletal vibration of aromatic benzene ring [1541 cm⁻¹]

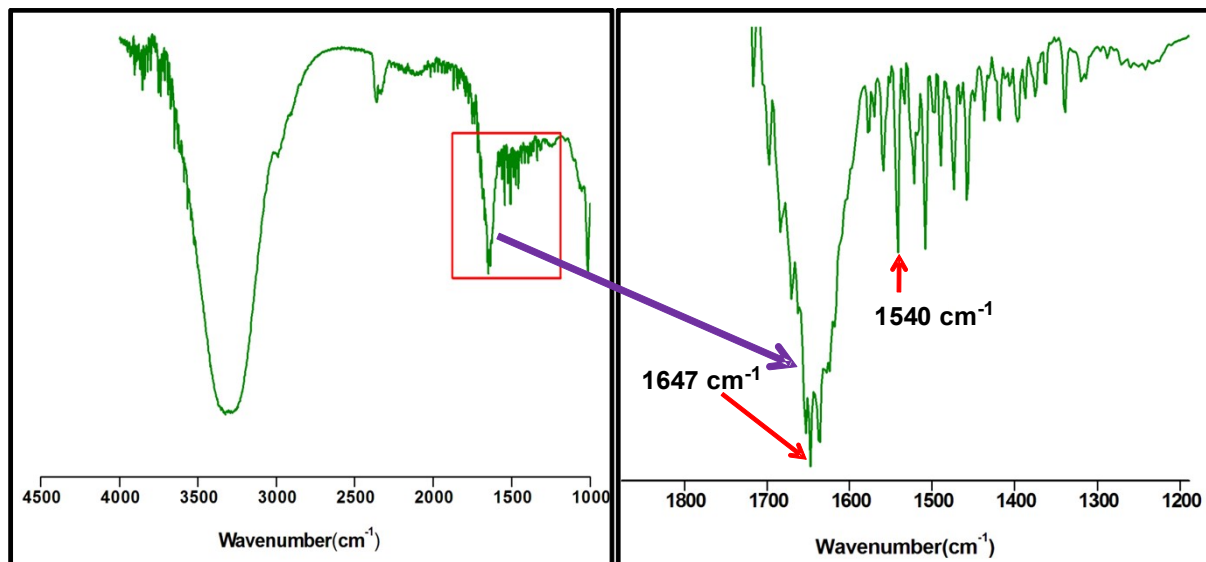
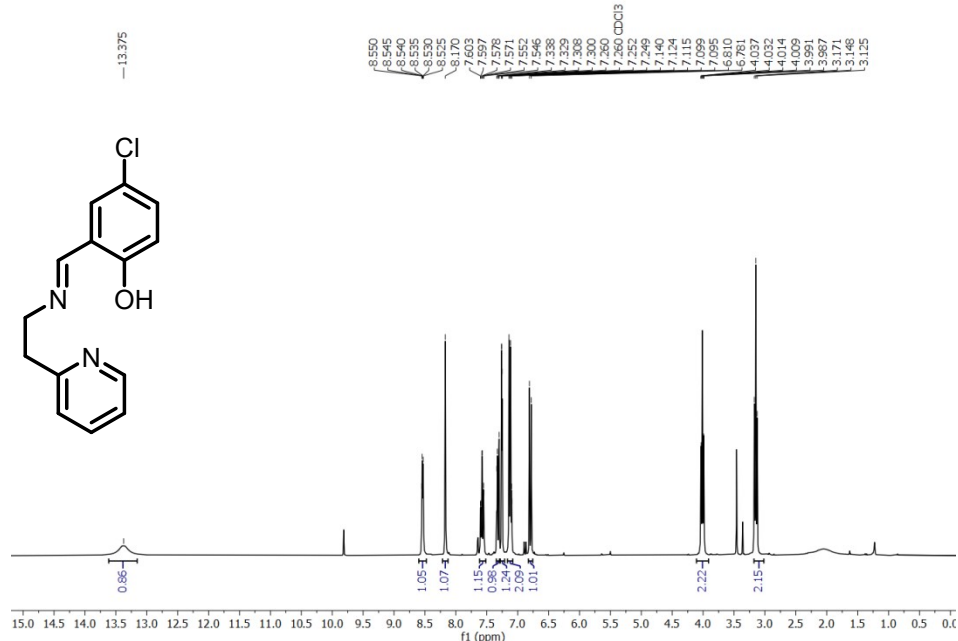
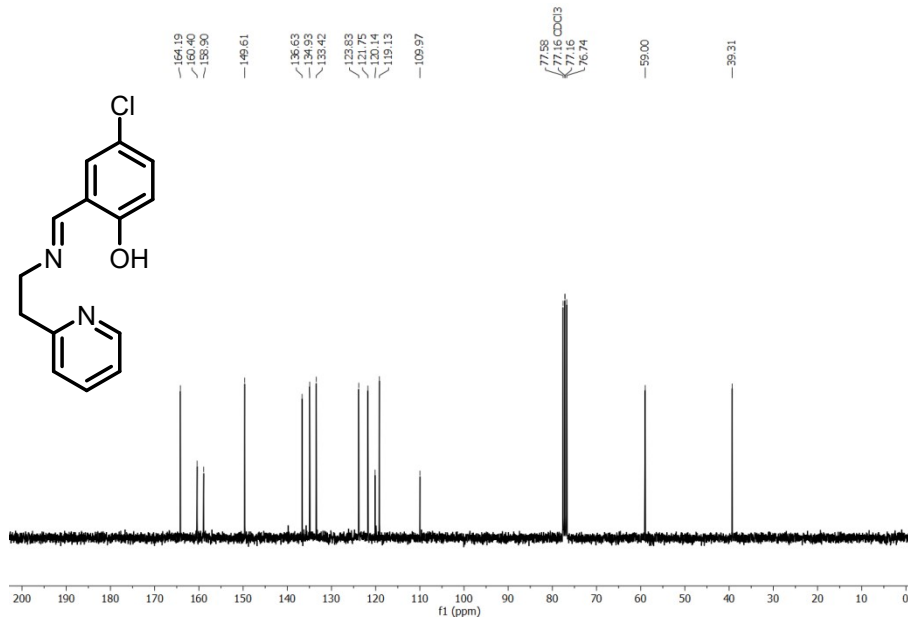


Fig. S2. FT-IR spectra of HL². Left, highlighted region is magnified to show the peaks due to C=N frequency [1647 cm⁻¹]; Right, skeletal vibration of aromatic benzene ring [1540 cm⁻¹].

4-chloro-2-(2-pyridyl)ethylimino)methylphenol (HL^1) : ^1H NMR (300 MHz, CDCl_3) δ 13.37 (s, 1H), 8.54 (dt, $J = 4.5, 1.5$ Hz, 1H), 8.17 (s, 1H), 7.57 (td, $J = 7.5, 1.8$ Hz, 1H), 7.32 (dd, $J = 9.0, 2.4$ Hz, 1H), 7.29 – 7.22 (m, 1H), 7.12 (dd, $J = 7.6, 4.8$ Hz, 2H), 6.80 (d, $J = 9.0$ Hz, 1H), 4.01 (td, $J = 6.9, 1.2$ Hz, 2H), 3.15 (t, $J = 6.9$ Hz, 2H) ppm. ^{13}C NMR (75 MHz, CDCl_3) δ 164.2, 160.4, 158.9, 149.6, 136.6, 134.93, 133.4, 123.8, 121.8, 120.1, 119.1, 110.0, 77.6, 77.1, 76.7, 59.0, 39.3 ppm.



(a)



(b)

Fig. S3. (a) ^1H NMR of 4-chloro-2-(2-pyridyl)ethylimino)methylphenol(HL^1)
(b) ^{13}C NMR of 4-chloro-2-(2-pyridyl)ethylimino)methylphenol(HL^1)

4-bromo-2-(2-pyridyl)ethylimino)methylphenol (HL^2) :

^1H NMR (300 MHz, CDCl_3) δ 13.34 (s, 1H), 8.56 – 8.53 (m, 1H), 8.18 (s, 1H), 7.61 – 7.55 (m, 1H), 7.20 (dd, $J = 9.0, 2.7$ Hz, 1H), 7.15 – 7.10 (m, 3H), 6.85 (d, $J = 9.0$ Hz, 1H), 4.06 – 3.98 (m, 2H), 3.16 (t, $J = 6.9$ Hz, 2H) ppm. ^{13}C NMR (75 MHz, CDCl_3) δ 164.3, 159.9, 158.9, 149., 136.6, 132.1, 130.4, 123.8, 123.1, 121.7, 119.5, 118.7, 77., 77.2, 76.7, 59.0, 39.3 ppm.

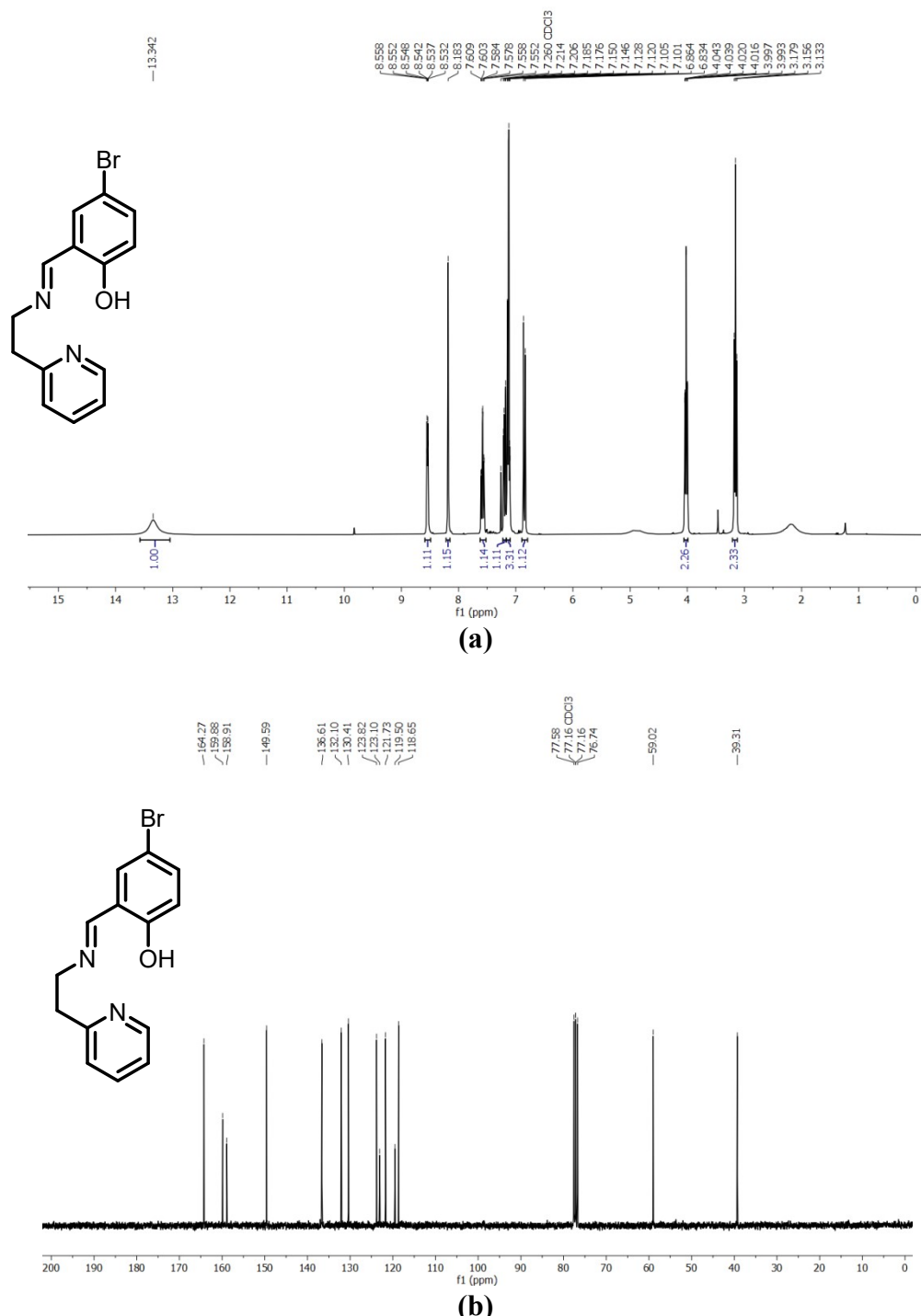


Fig. S4. (a) ^1H NMR of 4-bromo-2-(2-pyridyl)ethylimino)methylphenol(HL^2)
 (b) ^{13}C NMR of 4-bromo-2-(2-pyridyl)ethylimino)methylphenol(HL^2)

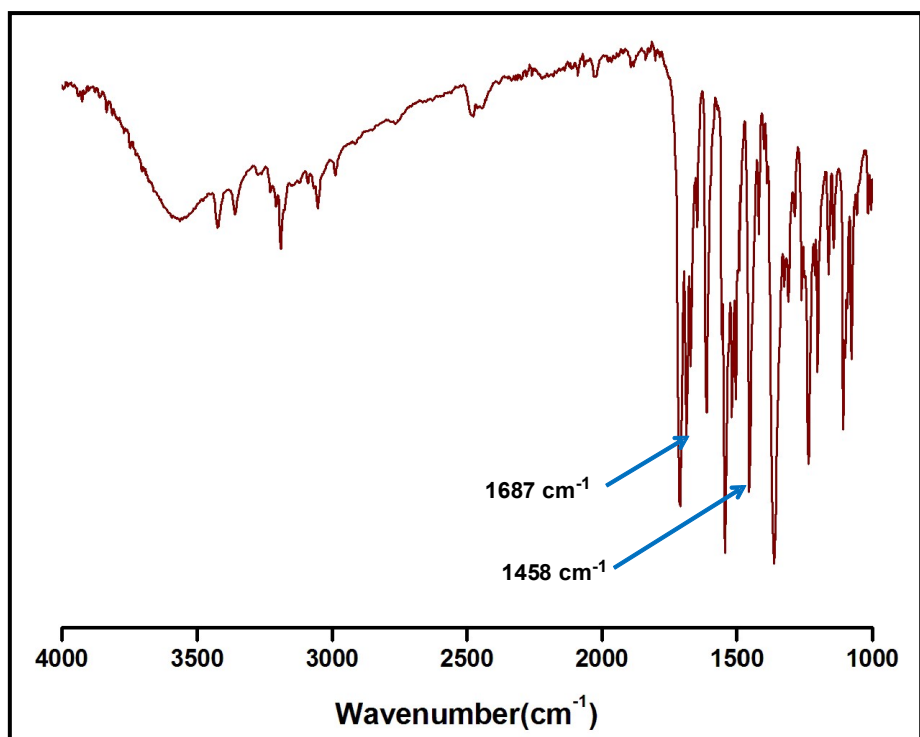


Fig. S5. FT-IR Spectrum of complex 1, $[\text{CuL}^1\text{Cl}]_2$

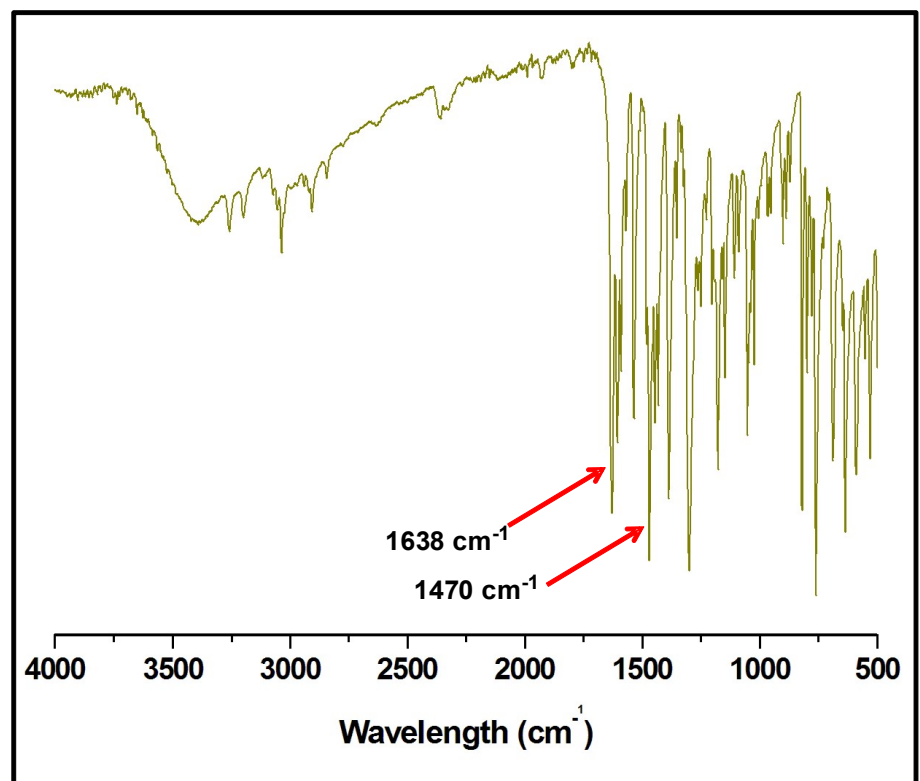


Fig. S6. FT-IR Spectrum of complex 2, $[\text{CuL}^2\text{Cl}]_2$

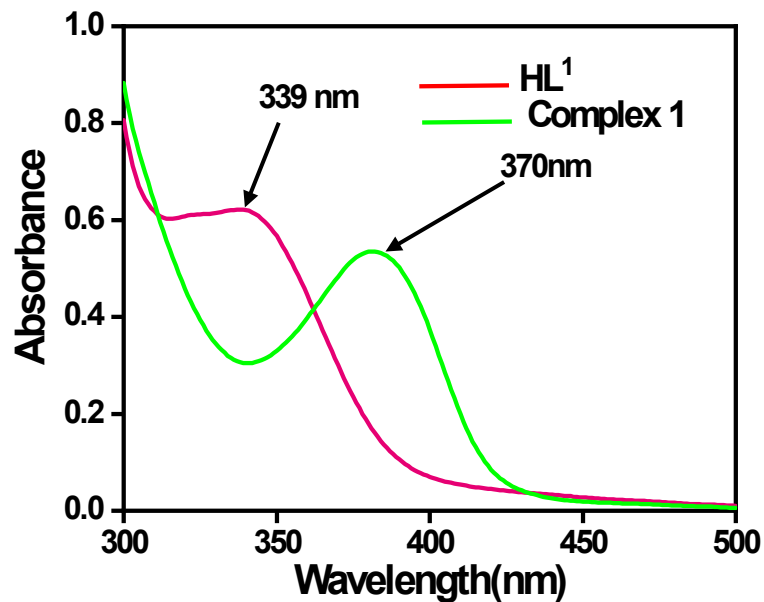


Fig. S7. UV Visible spectra of the ligand and complex **1**, $[\text{CuL}^1\text{Cl}]_2$

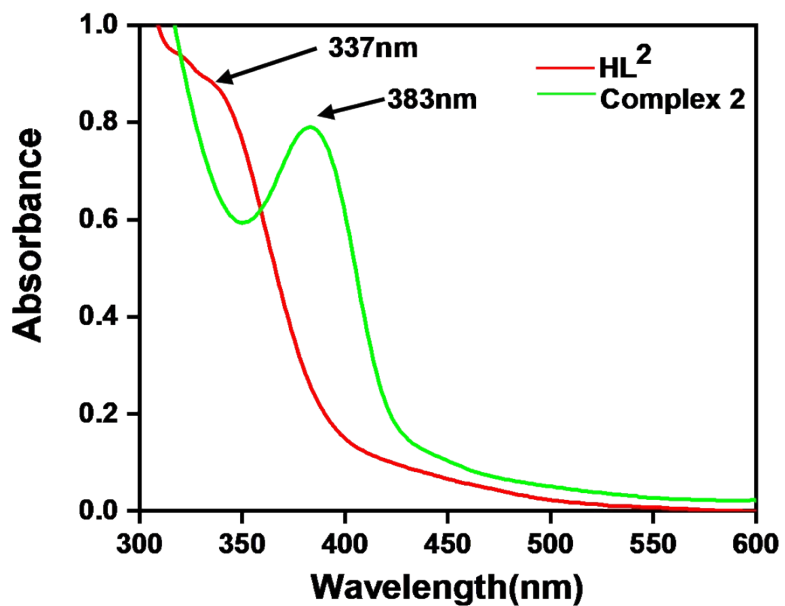
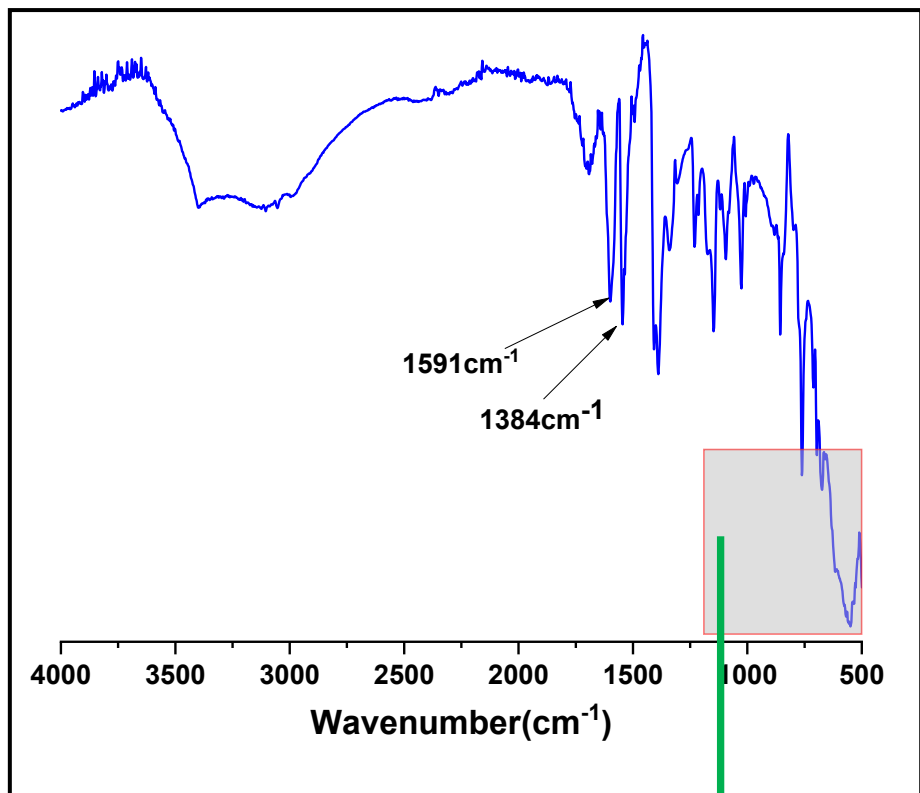
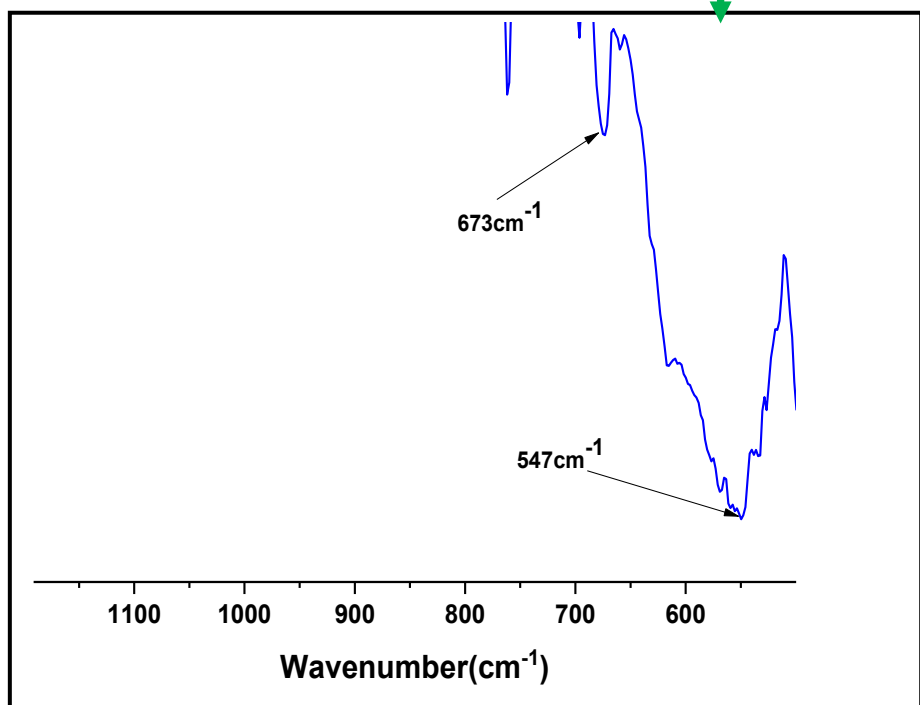


Fig. S8. UV Visible spectra of the ligand and complex **2**, $[\text{CuL}^2\text{Cl}]_2$



(a)



(b)

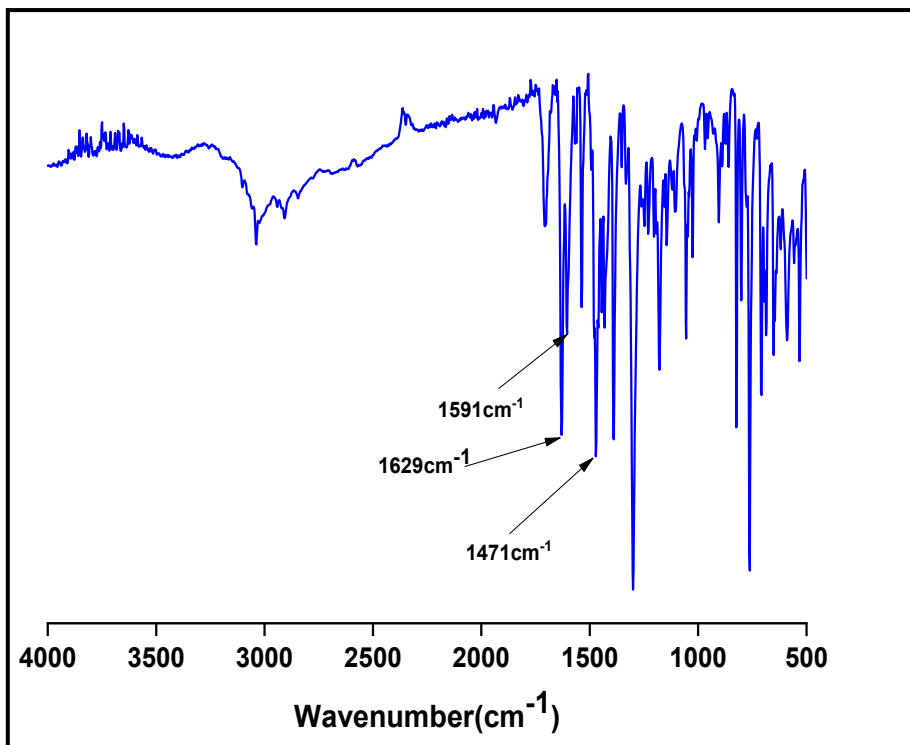


Fig. S9. FT-IR spectra of (a) $\text{Fe}_3\text{O}_4@\text{ISNA}$ (b) magnified portion highlighting FT-IR spectrum of $\text{Fe}_3\text{O}_4@\text{ISNA}$ (c) $\text{Fe}_3\text{O}_4@\text{ISNA}@\text{CuL}^1$

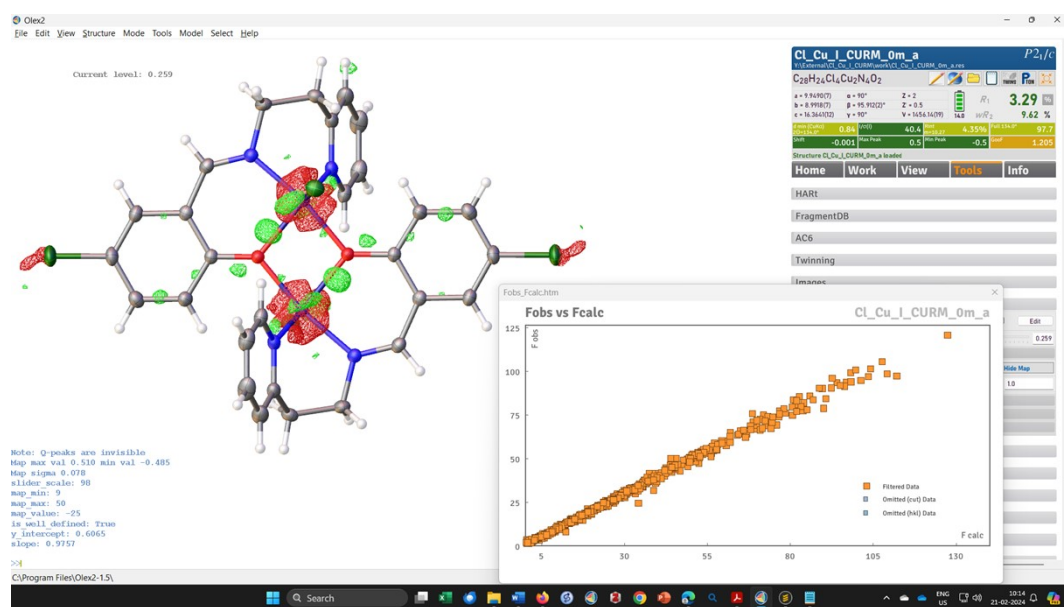


Fig. S10. The F_{obs} vs F_{calc} plot for complex **1** after suitably processed data.

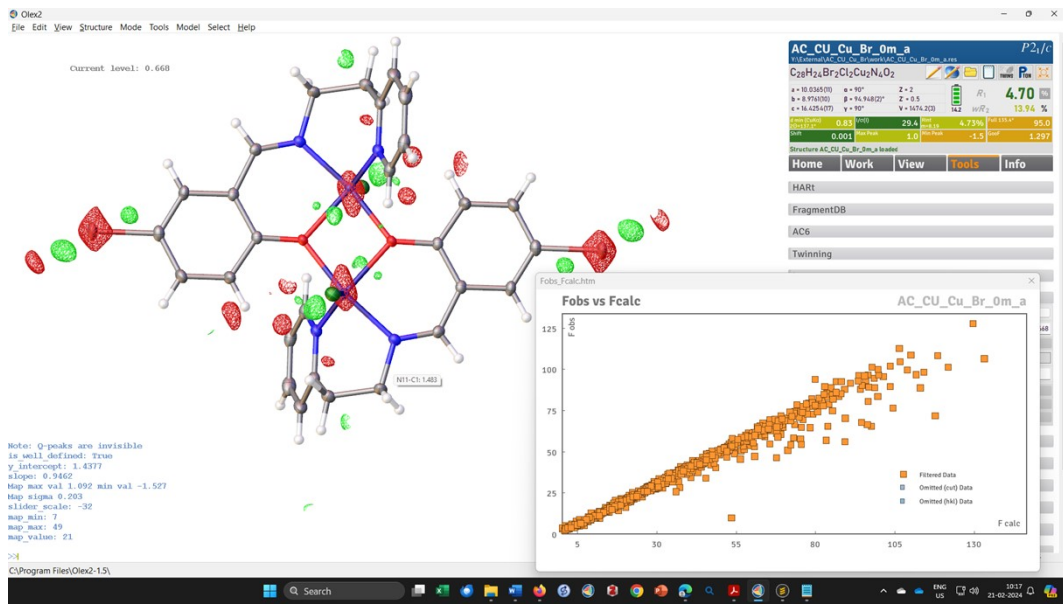


Fig. S11. The F_{obs} vs F_{calc} plot for complex **2** which reflects the crystal quality and consequently the diffraction pattern. When the crystal was cut, some microcrystals were on the edges, so that their diffraction might have contributed to the present observations where noisy reflections were observed in all batches (Fig. S12). The completeness of 95% was obtained by following the standard data collection time and redundancy. No reflection was omitted, no significant twin fraction was detected and no mistake or misassignment is associated with the structure.

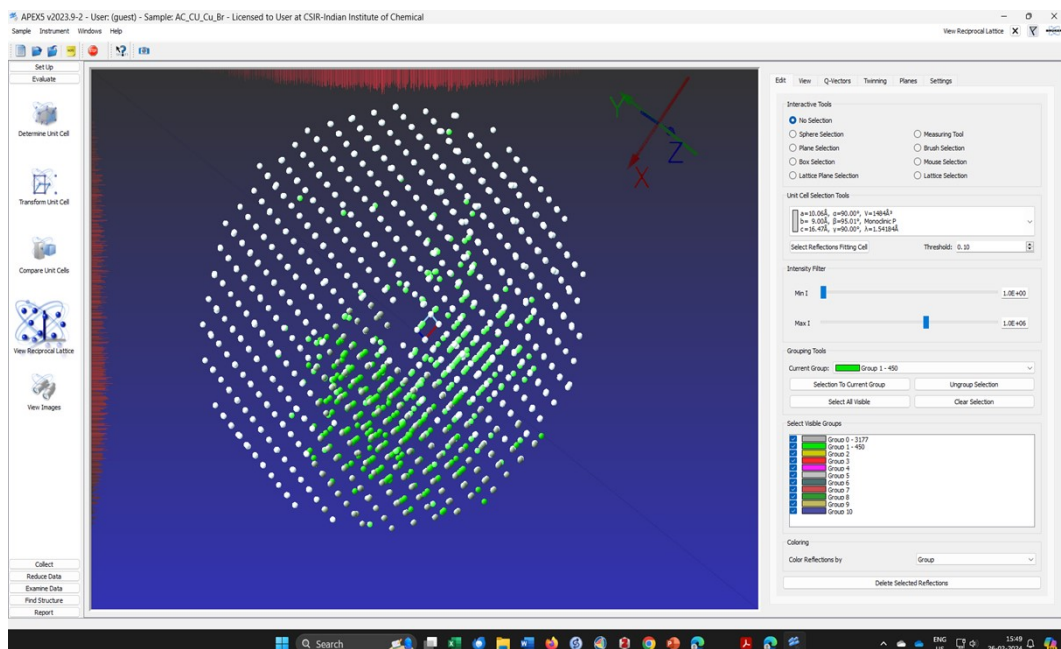


Fig. S12. View of reciprocal lattice for complex **2**. The green colour spots indicate reflections that do not fit into the major reflections and could not be indexed.

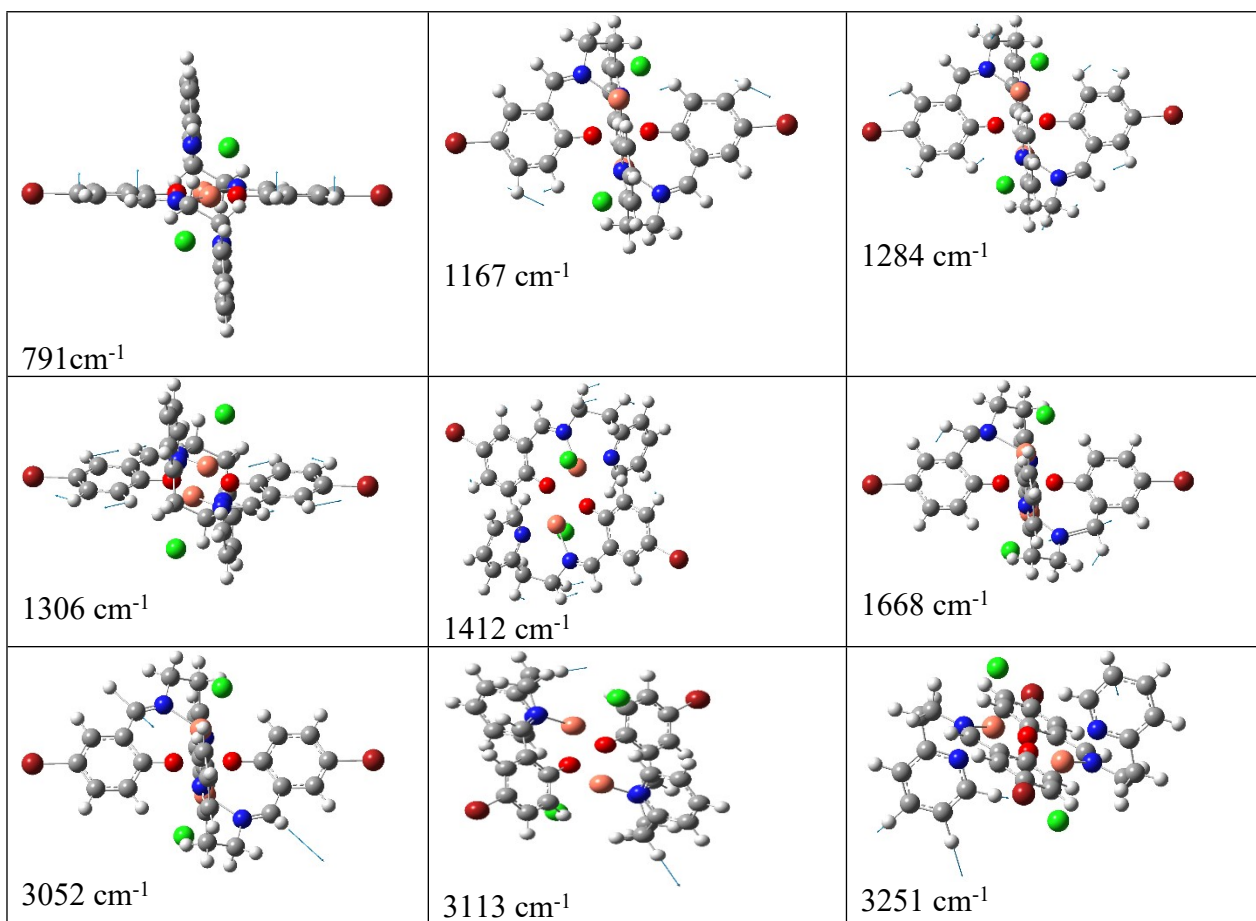


Fig. S13: Few selected different vibrational modes/motions of high intensity for complex **2**.

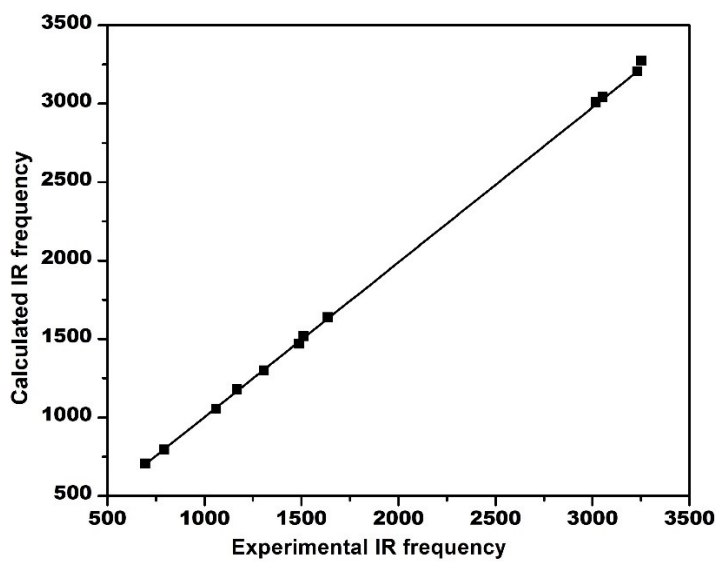


Fig. S14: Correlation of calculated and experimental frequencies of complex **2**.

Table 1S. Hydrogen bond parameters (\AA / $^\circ$) for complex **2**.

D-H	d(D-H)	d(H..A)	<DHA	d(D..A)	A	Symmetry code
C8-H8	0.95	2.76	159	3.666(3)	Cl1	1-x,1/2+y,3/2-z
C10-H10	0.95	2.70	157	3.594(3)	Cl1	1-x,1/2+y,3/2-z
C12-H12	0.95	2.80	166	3.727(3)	Cl1	1+x,y,z

Table 2S. Selected DFT calculated harmonic vibrational frequencies of complex **1** (a scaling factor of 0.96 was used above 2900 cm^{-1}) and of **2** and their band assignments.

Wavenumber (cm^{-1}) Complex 1	Intensity Complex 1	Wavenumber (cm^{-1}) Complex 2	Intensity Complex 2	Peak assignment
706	134	694	96	Benzene ring breathing
790	109	791	107	Op bending of C-H of benzene ring
1060	44	1061	42	C-N stretching
1166	69	1167	74	H-C=C-H scissoring in benzene ring
1238	41	1236	43	C(benzene)-C stretching
1278	176	1284	178	H-C=C-H scissoring in benzene ring coupled with twisting in H-C-H
1303	275	1306	459	H-C=C-H ip bending (rocking) in Benzene ring
1400	42	1401	75	H-C-H wagging CH2
1412	125	1412	105	H-C-H wagging CH2
1491	152	1488	209	H-C=C-H ip bending in benzene ring coupled with H-C-C-C scissoring
1495	94	1511	61	Ip bending of C-H of benzene ring
1572	119	1563	124	C=C stretching in benzene ring
1635	67	1636	60	C=C stretching in benzene ring
1664	385	1668	458	C=N stretching
3035	114	3016	114	H-C-H symmetric stretching
3077	135	3052	143	C(=N)-H stretching
3115	13	3113	71	Asymmetric H-C-H stretching
3230	11	3230	21	C-H asymmetric stretching in benzene ring
3249	26	3251	29	C-H symmetric stretching in benzene ring

Table 3S. The calculated absorption maxima, oscillator strength, and their corresponding band assignment for complex **1**.

Wavelength (nm)	Oscillator strength	Transition occurring from one MO to another MO	Assignment of band
388	0.0222	151 → 156	n(Cl/O)/ d _{xy} (Cu) → π*(benzene)
376	0.1504	149 → 153	π(benzene)/n(Cl/O) → π*(benzene)
370	0.0224	150 → 154	π(benzene)/n(Cl/O) → π*(benzene)/d _{x2-y2} (Cu)
357	0.0819	134 → 152	π(benzene)/ n(Cl/O) → d _{x2-y2} (Cu) π*(C=N)
355	0.0547	148 → 154	n(Cl) → π*(benzene)/ d _{x2-y2} (Cu)
346	0.0466	146 → 153	n(Cl) → π*(benzene)
305	0.0816	148 → 155	n(Cl/O) → π*(benzene)
304	0.0303	144 → 154	n(Cl/O)/π(benzene) → d _{x2-y2} (Cu)/ π*(benzene)
303	0.256	125 → 152	n(Cl, N)/π(benzene) → d _{x2-y2} (Cu) π*(C=N)

Table 4S. The calculated absorption maxima, oscillator strength, and their corresponding band assignment for complex **2**.

Wavelength (nm)	Oscillator strength	Transition occurring from one MO to another MO	Assignment of band
459	0.0063	142 → 152	π(benzene) → d _{x2-y2} (Cu)/n(Cl, N)
410	0.0132	151 → 156	n(Cl) → π*(benzene)
380	0.1571	149 → 153	π(benzene)/n(Br) → π*(benzene)
376	0.0305	150 → 154	π(benzene)/ n(Br/Cl) → π*(benzene)
368	0.0363	135 → 152	n(Br) → d _{x2-y2} (Cu)/n(Cl, N)
322	0.1605	126 → 152	π(benzene)/ n(Cl) → d _{x2-y2} (Cu)/n(Cl, N)
315	0.0367	144 → 154	n(Cl/O) → π*(benzene)
304	0.2805	124 → 152	π(benzene) → d _{x2-y2} (Cu)/n(Cl, N)